

# Thermoalkalophilic recombinant esterase entrapment in chitosan/calcium/alginate-blended beads and its characterization

Çisem Tercan,<sup>a</sup> Yusuf Sürmeli<sup>b,c</sup> and Gülşah Şanlı-Mohamed<sup>a,b\*</sup> 

## Abstract

**BACKGROUND:** Esterases (EC 3.1.1.1), a class of hydrolases, degrade the ester bonds of lipids into alcohol and carboxylic acids and synthesize carboxylic ester bonds. They are used in a variety of biotechnological, industrial, environmental, and pharmaceutical applications due to their many valuable properties. Particularly, extremophilic esterases with many superior properties are of great interest for various reactions. Immobilization of enzymes may provide some advantages over free enzymes not only to improve the properties of enzymes but also to increase the reusability of biocatalyst in industrial applications. Therefore, many different immobilization applications for enzymes have been reported in various studies. To our knowledge, a thermophilic esterase has not so far been immobilized by entrapment using chitosan/calcium/alginate-blended beads. Here, we reported the immobilization of thermoalkalophilic recombinant esterase by entrapment using chitosan/calcium/alginate-blended beads, and then the entrapped esterase was characterized biochemically in details.

**RESULTS:** In the present study, a thermophilic recombinant esterase was immobilized by entrapment in chitosan/calcium/alginate-blended beads for the first time. The 0.5 mg mL<sup>-1</sup> purified recombinant esterase was entrapped in 1% chitosan, 2% alginate, and 0.7 M CaCl<sub>2</sub> blended beads. The results showed that immobilization yield and entrapment efficiency of the entrapped esterase were 69.5% and 80.4%, respectively. SEM micrograph showed that the surface of the beads resembled a mesh and very compact structures. Chitosan/calcium/alginate-blended beads exhibited an 18.8% swelling ratio and had a moderate porous structure. The entrapment technique highly enhanced the thermostability of the esterase and shifted its optimum temperature from 65 to 80 °C. The immobilized esterase was very stable in a wide range of pH (8.5–11) displaying maximum activity at pH 9. ZnCl<sub>2</sub> slightly increased the activity of immobilized esterase whereas several metal ions reduced the enzyme activity. When the enzyme was immobilized in chitosan/calcium/alginate-blended beads, its K<sub>m</sub> increased about 2 times and V<sub>max</sub> value decreased almost 1.5 times. Immobilization allowed repeated uses of the esterase having good operational stability in a continuous process.

**CONCLUSION:** The results revealed that the immobilization of a thermophilic recombinant esterase by entrapment in chitosan/calcium/alginate-blended beads exhibited considerably better compared to other immobilization processes with various entrapment strategies.

© 2021 Society of Chemical Industry (SCI).

**Keywords:** esterase; *Geobacillus* sp; immobilization; entrapment; chitosan/calcium/alginate-blended bead

## INTRODUCTION

Enzymes are usually a great tool in a broad range of applications in biotechnological, biomedical, pharmaceutical, and industrial fields because they have essential catalytic features. However, the use of their free forms is not often optimal and convenient for these processes due to their poor stability, the inhibition effect of high substrate/product concentrations, and poor selectivity/activity to unnatural substrates under unconventional conditions. Immobilization technology of enzymes may be a powerful approach to improve these properties and to increase the reusability of biocatalyst in various reaction cycles of industrial processes. Enzyme immobilization may allow some additional advantages over free enzymes, such as fast reaction termination, ease of enzyme recovery from the reaction mixture, controlled end product generation, and possible continuity of the process.<sup>1,2</sup>

Different immobilization techniques are present using various support materials and methods.<sup>3–5</sup> Among these, entrapment is very straightforward for biocatalyst immobilization under moderate conditions relative to other immobilization techniques.<sup>6</sup>

\* Correspondence to: G Şanlı-Mohamed, Izmir Institute of Technology, Science Faculty, Department of Chemistry, Urla, Izmir, Turkey. E-mail: gulsahsanli@iyte.edu.tr, gulsahsanli@gmail.com

a Department of Chemistry, Izmir Institute of Technology, Izmir, Turkey

b Department of Biotechnology and Bioengineering, Izmir Institute of Technology, Izmir, Turkey

c Department of Agricultural Biotechnology, Tekirdağ Namık Kemal University, Tekirdağ, Turkey

Calcium alginate beads are one of the most frequently used carriers in the immobilization of enzymes by entrapment because they have some advantages including cost-effective, favorable biocompatibility, high stability against microbial attack, and availability.<sup>7</sup> Nevertheless, calcium alginate as a carrier has some obstacles such as enzyme leakage from beads, big pore size, and poor mechanical strength.<sup>8</sup> Additional techniques such as coating the surface of alginate beads with cross-linked biopolymers have been suggested to improve entrapment efficiency.<sup>9–13</sup>

In literature, several studies have reported different immobilization applications using chitosan/calcium/alginate beads on bacterial cell encapsulation, encapsulation of protein-stabilized lipid droplets, biosorption of phenol and *o*-chlorophenol, an oil-in-water emulsion containing allyl isothiocyanate, and insulin encapsulation for oral delivery.<sup>14–18</sup> Among these studies, Huang *et al.* have shown that *Lactobacillus reuteri* encapsulated in chitosan/calcium/alginate beads had a higher adherence rate than that in calcium alginate.<sup>14</sup> Kim *et al.* have also reported that the chitosan/calcium/alginate complex had the highest stability, compared to calcium alginate.<sup>17</sup>

Esterases (EC 3.1.1.1), which fall within a class of hydrolases, degrade the ester bonds of lipids into alcohol and carboxylic acids and synthesize carboxylic ester bonds. They are produced by many different organisms, such as animals, plants, and microorganisms.<sup>19</sup> The esterases act an important part in various biotechnological, industrial, environmental, and pharmaceutical applications due to their many valuable characteristics.<sup>20,21</sup> Particularly, extremophilic esterases with superior properties are of great interest in different reactions.<sup>22–24</sup> Thermoalkalophilic esterases can work at higher performance in some commercial applications relative to other enzymes since they have high thermal and alkaline stability.<sup>9</sup>

Recently, many studies have been reported various practices of esterase immobilization using different methods in literature.<sup>25,26</sup> Among these, *Mucor miehei* esterase was immobilized on core-shell magnetic beads by adsorption and covalent binding for ester synthesis.<sup>27</sup> Another esterase BioH was immobilized on a hydrophilic-modified solid support through oriented adsorption.<sup>28</sup> In addition, the esterase BioH from *Escherichia coli* was immobilized onto hydrophilic-modified magnetic nanosupport *via* oriented covalent immobilization.<sup>29</sup> Also, a novel cold-adapted esterase was immobilized on mesoporous silica SBA-15 by the absorption method.<sup>30</sup> Also, it has been immobilized by entrapment method using calcium-alginate for the first time and calcium-alginate beads were coated with silicate to overcome any leakage of the entrapped enzyme.<sup>9</sup> However, to the best of our knowledge, a thermophilic esterase has not been immobilized by entrapment using chitosan/calcium/alginate-blended beads in literature so far. Here, we reported the immobilization of thermoalkalophilic recombinant esterase by entrapment using chitosan/calcium/alginate-blended beads, and then the entrapped esterase was characterized biochemically. Eventually, the immobilization method for esterase by entrapment using chitosan/calcium/alginate-blended beads exhibited considerably better properties compared to another way of entrapment strategies.

## MATERIALS AND METHODS

### Materials

Unless otherwise stated all chemicals were purchased from Sigma.

### Enzyme preparation

Expression of the recombinant esterase from *Geobacillus* sp. previously isolated from reinjection water of Balçova

(Agamemnon) geothermal site in İzmir of Turkey<sup>31</sup> was performed in *Escherichia coli* BL21 ( $\Delta$ DE3). The purification of the enzyme by affinity chromatography was applied as stated in Tekedar and Şanlı-Mohamed (2011) procedure.<sup>32</sup> Then, the recombinant esterase was further purified by size-exclusion chromatography using a Sephadex G-75 column (Sigma). The purified enzyme was checked by 15% SDS-PAGE.<sup>33</sup> Protein concentration was determined by the Bradford method, using bovine serum albumin (BSA) standard solutions.<sup>34</sup>

### Immobilization of recombinant esterase into chitosan/calcium/alginate-blended beads

#### Obtaining chitosan-calcium chloride solution

Chitosan was synthesized from chitin using the method of Rigby and Wolfrom with some modification as described by İlgü *et al.* (2011).<sup>35</sup> The degree of deacetylation of chitosan was investigated by a LECO-CHNS-932 elemental analyzer (Monchengladbach, Germany) and it was calculated as about 87.3%. Also, molecular weight of chitosan was investigated by a viscosimetric method at the room temperature<sup>36</sup> and it was found in the range of middle molecular weight category. For preparation of chitosan-calcium chloride solution, 1% (w v<sup>-1</sup>) chitosan flakes were resuspended with 2% (v v<sup>-1</sup>) acetic acid at 50 °C. Then, 0.7 M CaCl<sub>2</sub> was supplemented into the chitosan solution and the mixture was stirred at 50 °C for 1 h.

#### Preparation of alginate-esterase solution

2% (w v<sup>-1</sup>) alginate was resuspended in 10 mL of 0.1 M Tris-HCl buffer (pH 8.0) at 30 °C for 30 min. 0.5 mg mL<sup>-1</sup> esterase enzyme was supplemented on the alginate solution and then the mixture was stirred for 1 h.

#### Formation of chitosan/calcium/alginate-blended beads with esterase

Alginate-esterase was dripped into 100 mL of chitosan-calcium chloride solution using a syringe during stirring the solution and white opaque chitosan/calcium/alginate-blended beads with esterase were formed. The size of beads was adjusted by syringes including different needle diameters. Solid beads were isolated from the solution using vacuum filtration. The beads were washed twice using dH<sub>2</sub>O and stored in 0.1 M Tris-HCl buffer (pH 8.0) at 4 °C for further analyses. Entrapment efficiency (EE) and Immobilization yield (IY) of the enzyme was determined using equations below:

$$EE = \frac{\text{total esterase} - \text{free esterase}}{\text{total esterase}} \times 100 \quad (1)$$

$$IY = \frac{\text{specific activity of immobilized esterase}}{\text{specific activity of free esterase}} \times 100 \quad (2)$$

#### Swelling behavior and porosity of chitosan/calcium/alginate-blended beads

The swelling behavior of chitosan/calcium/alginate-blended beads was determined based on the solvent uptake by the beads. Pre-weighed ( $W_d$ ) 10 dry chitosan/calcium/alginate-blended beads were suspended in 100 mL of 0.1 M Tris-HCl buffer (pH 8.0) at 30 °C for 6 h. Then, the excess buffer of chitosan/calcium/alginate-blended beads was removed by filter paper and immediately the weights of swollen beads ( $W_s$ ) were measured. The 'weight change' was calculated and expressed as % swelling rate calculated by the following equation: % swelling rate = ( $W_s$

$-W_d)/W_d \times 100$ . The measurements were made in triplicate and average data was used for calculations.

The porosity of chitosan/calcium/alginate-blended beads was determined according to the liquid displacement method described by Dorati *et al.*<sup>37</sup> Briefly, the initial weight of 10 dry beads was measured ( $W_1$ ) and then the beads were immersed in anhydrous ethanol for 6 h. Then, the excess ethanol was removed by filter paper and the weight of the absorbing beads was subsequently determined ( $W_2$ ). The porosity of chitosan/calcium/alginate-blended beads was calculated with the following equation: Porosity =  $W_2 - W_1/\rho V$ , where  $\rho$  is the density of anhydrous ethanol, which is  $0.79 \text{ g cm}^{-3}$ ;  $V$  refers to the volume of the beads. The measurements were made in triplicate and average data was used for calculations.

### Characterization of the immobilized recombinant esterase

#### Standard activity assay of the free and immobilized recombinant esterase

The hydrolytic activity of the free and immobilized recombinant esterases was spectrophotometrically determined using *p*-nitrophenyl acetate (*p*NPA) substrate, which had one of the most efficient hydrolytic catalytic activity among different kind of *p*-nitrophenyl (*p*-NP) esters having different acyl chain lengths (C2–C16).<sup>32</sup> For the free enzyme, the assay mixture contained  $9.5 \mu\text{L}$  of  $50 \text{ mmol L}^{-1}$  *p*NPA,  $990 \mu\text{L}$  of Tris-Cl buffer (pH 8.0), and  $0.5 \mu\text{L}$  of  $2.4 \text{ mg mL}^{-1}$  enzyme solution, and enzyme activity was determined at  $55 \text{ }^\circ\text{C}$  for 5 min by  $\text{OD}_{420}$  measurement. For the immobilized enzyme activity, the reaction mixture had  $10 \mu\text{L}$  of  $50 \text{ mmol L}^{-1}$  *p*NPA,  $980 \mu\text{L}$  of Tris-Cl buffer (pH 8.0), and 10 beads (0.008 mg) of immobilized enzyme solution, and its activity was determined at  $55 \text{ }^\circ\text{C}$  for 5 min by  $\text{OD}_{420}$  measurement. One unit of esterase activity was defined as the amount of enzyme releasing 1 nmol of *p*-nitrophenol per minute.

#### Temperature and pH effect

The effect of temperature and pH on the free and immobilized recombinant esterase was observed using *p*-NPA as a substrate at 90 rpm. The temperature effect on the free and immobilized enzyme was analyzed in a wide range of temperatures ( $35\text{--}80 \text{ }^\circ\text{C}$ ) using  $0.1 \text{ M}$  Tris-Cl buffer (pH 8.0). The pH effect on the free and immobilized enzyme was investigated ranging from pH 4 to 11 at  $55 \text{ }^\circ\text{C}$ . Standard activity assay conditions were applied to determine the relative enzyme activity.

#### Temperature and pH stability

Temperature analysis for free and immobilized esterase was performed in a range of temperatures ( $40\text{--}80 \text{ }^\circ\text{C}$ ) for 1 h of preincubation using  $0.1 \text{ M}$  Tris-Cl buffer (pH 8.0). In addition, pH stability was investigated in a range of pH (4–11) at  $55 \text{ }^\circ\text{C}$ . The standard activity assay was applied to determine the residual enzyme activity.

#### Effect of chemicals

The effect of metal ions ( $1 \text{ mmol L}^{-1}$   $\text{CaCl}_2$ ,  $1 \text{ mmol L}^{-1}$   $\text{ZnCl}_2$ ,  $1 \text{ mmol L}^{-1}$   $\text{MgCl}_2$ , and  $1 \text{ mmol L}^{-1}$   $\text{CuSO}_4$ ) and two surfactants (1% SDS and 1% Triton X-100) was investigated for the free and immobilized esterase under standard activity assay conditions and relative activity was determined.

#### Kinetic studies

Kinetic parameters of free and immobilized thermoalkalophilic recombinant esterase were determined using Lineweaver–Burk

plots and assuming that the reactions followed a simple Michaelis–Menten kinetics. Lineweaver–Burk curves were obtained for *p*-nitrophenyl acetate (*p*NPA) at six different substrate concentrations ( $0.05, 0.1, 0.3, 0.5, 0.7$  and  $1 \text{ mmol L}^{-1}$ ) using standard enzyme assay.

#### Operational stability

Operational stability analysis was performed by the application of seven sequential standard activity assay of the immobilized enzyme. Following each assay, the beads were washed three times using  $\text{dH}_2\text{O}$ .

#### The influence of bead size

Chitosan/calcium/alginate-blended beads were created in three distinct sizes, using different sizes of a needle. The bead diameters were calculated, utilizing the formula below and then the standard activity assay was performed.

$$\text{increment in volume} = 4/3 \times \pi \times (\text{bead diameter})^3 \times \text{number of beads} \quad (3)$$

#### Scanning electron micrography (SEM) analysis

The bead qualities of the surface morphology and internal structure were investigated by scanning electron microscope (Phillips XL-30S FEG).

#### Data presentation and statistical analysis

All experiments were performed at least in duplicate. Statistical errors of the data were determined by GraphPad Prism version 6.00 for Windows (GraphPad Software, La Jolla, CA, USA) (www.graphpad.com).

## RESULTS AND DISCUSSION

In this study, thermoalkalophilic recombinant esterase was immobilized by entrapment in chitosan/calcium/alginate-blended beads. Heterologous expression of esterase enzyme was carried out in *Escherichia coli* BL21 (DE3) and the enzyme was purified homogeneously before the immobilization. Heterologous expression and purification of free esterase resulted in 30–40 mg of purified active protein with high specific activity.<sup>32</sup> The purity of the enzyme was checked by SDS-PAGE (Fig. 1).

#### Swelling behavior and porosity of chitosan/calcium/alginate-blended beads

Swelling behavior is an important parameter for hydrogel-type materials studies. Therefore, chitosan/calcium/alginate-blended beads as hydrogel were tested for their swelling property as an immobilization material for thermoalkalophilic recombinant esterase. The exhibited swelling ratio of the prepared chitosan/calcium/alginate-blended beads was obtained as 18.8%. The swelling behavior of the beads was a moderate swelling ratio and slightly lower than reported hydrogels in the literature.<sup>38–40</sup> The results may be ascribed to the formation of the beads and tested swelling conditions such as pH. It has been previously demonstrated that the percentage swelling of hydrogels in acidic solution was found to be higher than in alkaline solution.<sup>41</sup>

The porosity of chitosan /calcium/alginate-blended beads was evaluated by the liquid displacement method with ethanol which can penetrate into the pores materials without inducing shrinkage and swelling. The results displayed that the beads formed

by alginate and chitosan had a moderate porous structure and porosity was approximately 75%. The results obtained were also consistent with the previous studies.<sup>39,42</sup> As a result, the porous nature of the beads and their reasonable and good space may cause the thermoalkalophilic recombinant esterase to be entrapped with high loading capacity.

### Immobilization of thermoalkalophilic esterase on chitosan/calcium/alginate-blended beads

The 0.5 mg mL<sup>-1</sup> purified recombinant esterase was entrapped in 1% chitosan, 2% alginate, and 0.7 M CaCl<sub>2</sub> blended beads. The results showed that immobilization yield and entrapment efficiency of the entrapped esterase were 69.5% and 80.4%, respectively.

### Characterization of the immobilized thermoalkalophilic esterase

The immobilized thermoalkalophilic esterase was characterized by investigation of several parameters including pH effect, temperature effect, thermostability, the effect of various chemicals, operational stability, and effect of different bead size.

#### The influence of temperature and pH

The activities of both free and immobilized esterases were investigated in a range of temperatures (35 to 80 °C). Temperature effect analysis showed that free esterase had maximum activity at 65 °C. After immobilization of the esterase in chitosan/calcium/alginate-

blended beads, it was found that the optimum temperature for immobilized esterase was shifted to 80 °C (Fig. 2(a)). Thus, the immobilized esterase showed its catalytic activity at a higher reaction temperature by 15 °C compared to that of the free enzyme. In a previous study, the same esterase by entrapped in silicate-coated Ca-alginate beads and the immobilized enzyme in that study optimally worked at 70 °C,<sup>9</sup> lower than that of in the present study. This result could be interpreted that the entrapment way by chitosan/calcium/alginate-blended beads may limit enzyme physically within micro spaces of the beads to ease substrate diffusion to the active site at high temperatures. In literature, there have been many studies on different immobilization approaches of esterases from various sources. An immobilized esterase from *Zunongwangia* sp. in Fe<sub>3</sub>O<sub>4</sub> ~ cellulose nano-composite had an optimal temperature of 35 °C, higher 5 °C than free esterase.<sup>43</sup> Another esterase from *Lactobacillus plantarum* possessed maximum activity at 30 °C for free enzyme and 50 °C for its immobilized form on hydrophobic support polypropylene Accurel MP1000 by adsorption.<sup>44</sup> Also, an esterase from *Bacillus altitudinis* (Est<sub>BAS</sub>ΔSP) optimally worked at 50 °C, whereas its immobilized form of the enzyme (Lx-Est<sub>BAS</sub>ΔSP) onto an epoxy resin exhibited maximum activity at 60 °C.<sup>45</sup> A free and immobilized wheat esterase using glass fiber film optimally worked at 30 and 40 °C, respectively.<sup>46</sup> Additionally, free esterase from *Bacillus pumilus* and its immobilized form on silane functionalized superparamagnetic nanoparticles (SNPs) had maximum activity at 37 and 45 °C, respectively.<sup>47</sup> The esterase from *Lysinibacillus fusiformis* AU01 showed maximum activity at 40 °C for free enzyme and at 45 °C for immobilized enzyme onto celite545 with 3-aminopropyltriethoxysilane as a linker molecule.<sup>48</sup> Besides, free and immobilized *Mucor miehei* esterase on core-shell magnetic beads via adsorption and covalent binding showed an optimal temperature at 40 and 50 °C, respectively.<sup>27</sup> A free cold-adapted *Pseudomonas mandelii* esterase (rEstKp) and immobilized esterase by cross-linking (GO-rEstKp) showed a similar optimum temperature.<sup>49</sup> A free and immobilized esterase BioH on hydrophilic-modified solid support via oriented adsorption possessed optimum temperature at 50 °C.<sup>28</sup> The increase of 15 °C after immobilization in the present study showed that esterase entrapment by chitosan/calcium/alginate-blended beads resulted in a superior optimum temperature among the studies available in the literature. According to the results, we may suggest that the immobilization matrix obtained by chitosan/calcium/alginate blend might be able to protect the enzyme against denaturation at higher temperatures.

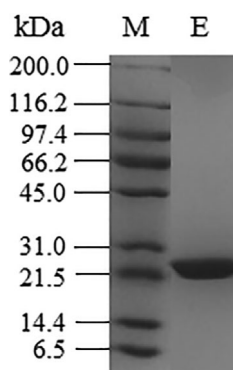


**Figure 1.** SDS-PAGE analysis of the purified recombinant thermoalkalophilic esterase from *Geobacillus* sp. E: purified Esterase, M: the protein marker.

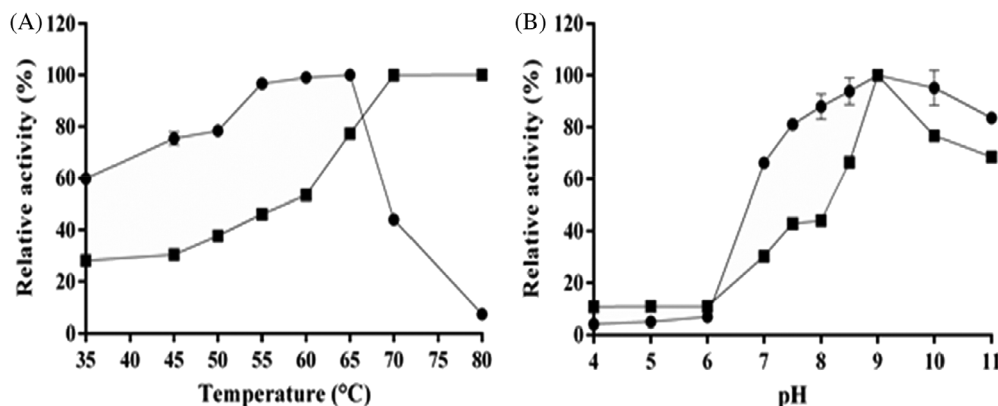


**Figure 2.** The influence of temperature (35–80 °C) (a) and pH (4–11) (b) of free esterase (●) and the immobilized esterase (■).

For pH effect, free and immobilized esterase activities were investigated in a range of pH 4 to 11. The pH effect results showed that free esterase exhibited maximum activity at pH 9. After immobilization of the esterase in chitosan/calcium/alginate-blended beads, the optimum pH did not change (Fig. 2(b)). The same esterase by entrapment in silicate-coated Ca-alginate beads optimally worked at pH 8,<sup>9</sup> lower than 1 pH unit, compared to the present study. Similar to our findings, several studies have shown that different immobilization techniques did not change the optimal pH values of esterases from various sources.<sup>43,45,49</sup> Besides, immobilization of wheat esterase on glass fiber film decreased optimum pH by one unit, compared to the free form.<sup>46</sup> In contrast, immobilization of *Mucor miehei* esterase on core-shell magnetic beads increased the optimum pH by one unit, compared to its free form.<sup>27</sup>

#### Thermal stability

The thermal stability of free and immobilized esterase was investigated in a range of temperatures (40–80 °C) upon 1 h of incubation. Thermostability results showed that the immobilized esterase had the highest residual activity at 60 °C, slightly more than that in free esterase. However, free esterase activity sharply dropped at 70 and 80 °C, showing 61% and 6% of residual activity, respectively. Indeed, the immobilized enzyme maintained high residual activity as 92% at 70 °C and 80% at 80 °C after 1 h of incubation (Fig. 3). The thermoalkalophilic recombinant esterase in a previous study immobilized in silicate-coated Ca-alginate beads had a residual activity of about 60% at 80 °C upon 1 h of incubation.<sup>9</sup> The present study showed that esterase immobilization by chitosan/calcium/alginate-blended beads displayed superior thermal stability compared to silicate-coated Ca-alginate beads. This phenomenon could be related to the location of esterase inside the immobilization support. The conformational movement of esterase might be restricted inside the immobilization matrix so that enzyme may be protected against its denaturation at high temperatures for a while. Comparable results have been reported in some studies about the thermal stability of immobilized esterases. Accordingly, an immobilized esterase on hydrophobic support polypropylene Accurel MP1000 by adsorption was highly stable at 80 °C after 60 min of incubation, exhibiting 100% of residual activity.<sup>44</sup> In addition, an immobilized esterase CLEA-LpSGNH1 completely conserved almost all its activity at 60 °C throughout 60 min, whereas free esterase LpSGNH1 completely lost its activity.<sup>50</sup> An immobilized esterase Lx-Est<sub>BAS</sub>ΔSP also showed higher stability than free esterase Est<sub>BAS</sub>ΔSP and retained

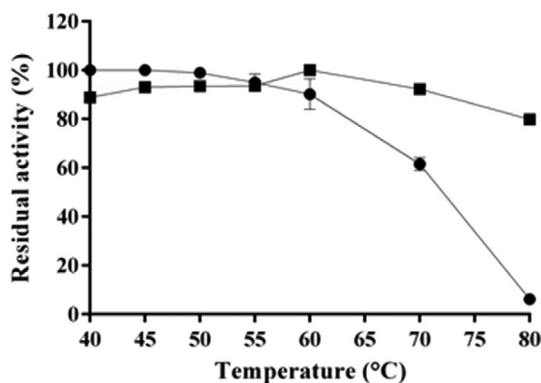


**Figure 3.** Thermal stability of free esterase (●) and immobilized esterase (■) at the range of 40–80 °C after 60 min of incubation.

about 80% of residual activity at 60 °C after 1 h of incubation.<sup>45</sup> Furthermore, two immobilized *Mucor miehei* esterase on core-shell magnetic beads *via* adsorption and covalent binding showed 80% and 90% of residual activity at 60 °C, respectively.<sup>27</sup> There have been reported some studies on the thermal stability of free and immobilized esterase from various sources, showing much lower thermal stability, compared to the present study. In line with this, the activities of free and immobilized esterase in Fe<sub>3</sub>O<sub>4</sub> ~ cellulose nano-composite decreased below 20% at 50 °C after 60 min.<sup>43</sup> Also, immobilized esterase G on amine-functionalized supports retained a residual activity of about 70% at 65 °C after 1 h of incubation, whereas free esterase G did not show any activity.<sup>51</sup> Besides, the immobilized esterases GO-rEstKp and CPE-SuIE completely lost their residual activities at 60 °C after 60 and 30 min, respectively, although they exhibited higher thermal stability than their free forms.<sup>49,52</sup>

The pH stability of immobilized esterase was studied in a variety of pH (4–11) for 1 h of incubation. The analysis results showed that immobilized esterase was very stable between pH 8.5–11, retaining almost all its activity after 1 h, whereas it had low stability at acidic and neutral pH conditions (data not shown).

#### Effect of chemicals

The effect of different chemicals on free and immobilized esterases was investigated in the presence of each metal ion (CaCl<sub>2</sub>, ZnCl<sub>2</sub>, MgCl<sub>2</sub>, CuSO<sub>4</sub>, and MgSO<sub>4</sub>) at 1 mmol L<sup>-1</sup> concentration and two surfactants (SDS and Triton X-100) at 1% concentration. This analysis results showed that ZnCl<sub>2</sub> slightly increased the activity of immobilized esterase whereas, CaCl<sub>2</sub> did not change. However, the other metal ions MgCl<sub>2</sub>, CuSO<sub>4</sub>, and MgSO<sub>4</sub> reduced the immobilized esterase activity by 25%, 13%, and 4%, respectively (Fig. 4). In literature, the activity of an immobilized esterase from *Neisseria meningitides* on hybrid nanoflowers (hNF-NmSGNH1) was increased by Cu<sup>2+</sup> whereas it dramatically dropped in the presence of Ca<sup>2+</sup>.<sup>53</sup> Besides, immobilized esterase Lx-Est<sub>BAS</sub>ΔSP activity was reduced by 3% in the presence of Zn<sup>2+</sup> whereas Mg<sup>2+</sup> increased its activity by 8%.<sup>45</sup> The surfactant analysis result showed that SDS completely inhibited the immobilized esterase activity whereas Triton X-100 strongly decreased by 42% (Fig. 4). Similarly, immobilized esterase in Fe<sub>3</sub>O<sub>4</sub> ~ cellulose nano-composite lost almost all of its activity in the presence of

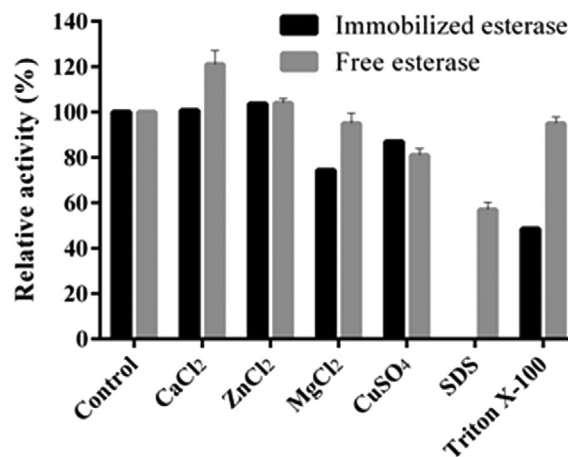


**Figure 4.** The influence of metal ions at 1 mmol L<sup>-1</sup> concentrations and two surfactants (1% SDS and 1% Triton X-100) on the free and immobilized esterase.

SDS and dropped by about 70% in the presence of Triton X-100.<sup>43</sup> Also, CLEA-estUT1 activity was reduced as much as 70% by Triton X-100 whereas SDS did not change its activity.<sup>54</sup> Additionally, 1%

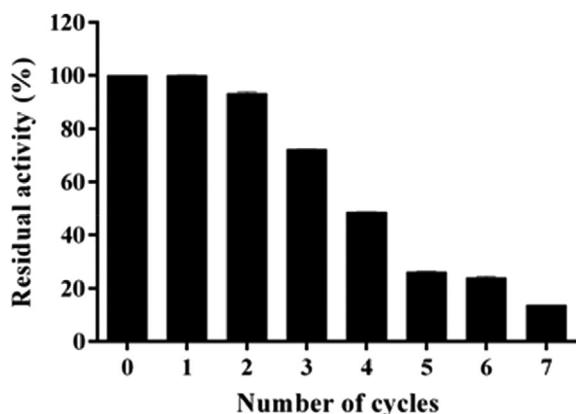


**Figure 5.** Operational stability of the immobilized esterase at seven sequential cycles.

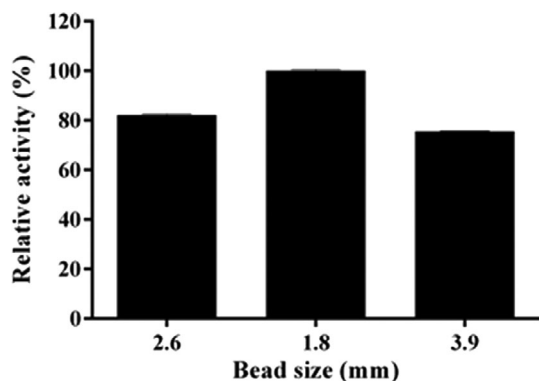


**Figure 6.** The influence of three different diameters of beads (1.8, 2.6, and 3.9 mm) on immobilized esterase activity.

SDS inhibited almost all of its activity of the immobilized esterase from *Paenibacillus* sp. (CLEAs-PsEstA).<sup>55</sup> The activity of another immobilized esterase from *Neisseria meningitides* on crosslinked enzyme aggregates (NmSGNH1-CLEAs) was slightly reduced by Triton X-100; however, it was dramatically dropped by SDS.<sup>53</sup> In another study, SDS and Triton X-100 dramatically reduced immobilized esterase LX-Est<sub>BAS</sub>ΔSP activity by 80% and 62%, respectively.<sup>45</sup>

#### Kinetic studies

The kinetic parameters  $K_m$  and  $V_{max}$  for free and immobilized esterase were determined by using p-nitrophenyl acetate (pNPA) substrate concentration from 0.05 to 1 mmol L<sup>-1</sup> in the reaction mixture. Both free and immobilized thermoalkalophilic recombinant esterase exhibited a simple Michaelis–Menten kinetics and Lineweaver–Burk plot showed a linear response over the tested concentration range. The  $K_m$  value of immobilized esterase was estimated to be 0.44 mmol L<sup>-1</sup> which was slightly higher than that of the free enzyme (0.26 mmol L<sup>-1</sup>). The structural changes in the enzyme and/or steric limitations introduced by the immobilization may be attributed to this change as the reduction in the enzyme affinity for its substrate.<sup>56,57</sup> The  $V_{max}$  values of free and immobilized thermoalkalophilic recombinant esterase were estimated to be 19.02 and 12.85 mmol L<sup>-1</sup> mL<sup>-1</sup> min<sup>-1</sup>, respectively. It has been known that a decrease in the  $V_{max}$  value during the immobilization process is commonly observed because of limitations on diffusion.<sup>9,58</sup> Similar results were also observed with other studies of esterases from various sources.<sup>29,52</sup>

#### Operational stability

The operational stability of an immobilized enzyme is a very important parameter for the application of enzyme in large scale processes in order to reduce the operation cost. Therefore, the operational stability of immobilized esterase was tested as several enzymatic reaction cycles performed in 0.1 M Tris–HCl buffer (pH 8.0) at 55 °C and 90 rpm for 5 min in the presence of p-NPA as substrate. The specific activity of the immobilized enzyme was detected following each cycle of the enzymatic reaction and the residual activity was determined. The results showed that

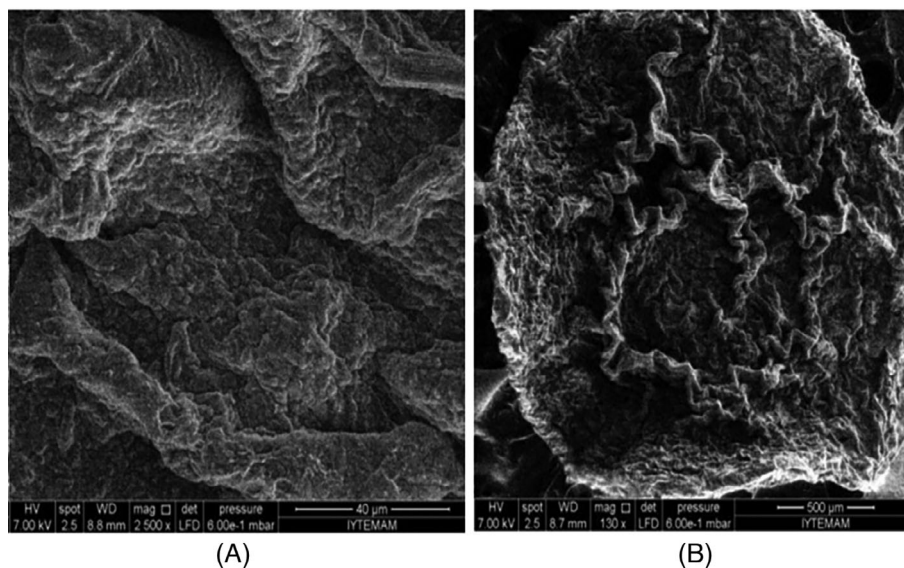


**Figure 7.** Surface morphology of the immobilized esterase in SEM micrograph by the magnitude of 2500× (a) and 40× (b).

the immobilized esterase maintained about 72% of its residual activity after three sequential cycles, indicating that it has good operational stability (Fig. 5). Gülay and Şanlı-Mohamed (2012) have reported that the same esterase by entrapment in silicate-coated Ca-alginate beads had more than 80% of the enzyme activity after three subsequent cycles.<sup>9</sup> There have been some recent reports with similar results on immobilized esterases using different techniques, showing at least 70% of residual activity after three sequential cycles.<sup>45,47,53,55,59,60</sup>

#### The influence of bead size

The effect of bead sizes (1.8, 2.6, and 3.9 mm) was investigated on the activity of the immobilized enzyme. This analysis results showed that the highest esterase activity was determined at 1.8 mm diameter beads the smallest size obtained in the present study (Fig. 6). The same esterase by entrapment in silicate-coated Ca-alginate beads had maximum activity at 0.5 mm bead size.<sup>9</sup>

#### Surface morphology of the immobilized esterase

The surface morphology of dried chitosan/calcium/alginate-blended beads with esterase was monitored by scanning electron microscopy (SEM) at magnitudes of 2500x and 40x. SEM micrograph showed that the surface of the beads resembled a mesh and very compact structures (Fig. 7(a), (b)).

## CONCLUSIONS

To conclude, the immobilization of enzymes may offer some advantages over free enzymes in industrial applications. In this study, we immobilized recombinant thermoalkalophilic esterase enzyme from Balçova geothermal site, because of the great interest of esterase in various biotechnological applications. Thanks to the present study, a thermophilic esterase was, for the first time, immobilized by entrapment using chitosan/calcium/alginate-blended beads. The analysis results revealed that chitosan/calcium/alginate-blended beads resulted in 69.5% of immobilization yield and 80.4% of entrapment efficiency. SEM micrograph showed that the surface of the beads resembled a mesh and very compact structures. Chitosan/calcium/alginate-blended beads exhibited an 18.8% swelling ratio and had a moderate porous structure. The entrapment technique highly enhanced the thermostability of the esterase and shifted its optimum temperature from 65 to 80 °C. The immobilized esterase was very stable in a wide range of pH (8.5–11) displaying maximum activity at pH 9. ZnCl<sub>2</sub> slightly increased the activity of immobilized esterase whereas several metal ions reduced the enzyme activity. Immobilized enzyme presented lower  $V_{max}$  and higher  $K_m$  than free enzyme. Additionally, immobilization technique allowed repeated uses of the esterase having good operational stability in a continuous process.

## ACKNOWLEDGEMENT

The authors would like to thank Biotechnology & Bioengineering Research Center at İzmir Institute of Technology for the facilities and technical support.

## REFERENCES

- Ozalp VC, Bayramoglu G and Arica MY, Fibrous polymer functionalized magnetic biocatalysts for improved performance, in *Methods in Enzymology*, Vol. 630. Academic Press Inc, United States, pp. 111–132 (2020).
- Tischer W and Kasche V, Immobilized enzymes: crystals or carriers? *Trends Biotechnol* **17**:326–335 (1999).
- Bayramoglu G, Salih B and Yakup Arica M, Catalytic activity of immobilized chymotrypsin on hybrid silica-magnetic biocompatible particles and its application in peptide synthesis. *Appl Biochem Biotechnol* **190**:1224–1241 (2010).
- Bayramoglu G, Kayili HM, Oztekin M, Salih B and Arica MY, Hydrophilic spacer-arm containing magnetic nanoparticles for immobilization of proteinase K: employment for speciation of proteins for mass spectrometry-based analysis. *Talanta* **206**:120218 (2020).
- Ozyilmaz G and Yagiz E, Isoamylacetate production by entrapped and covalently bound *Candida rugosa* and porcine pancreatic lipases. *Food Chem* **135**:2326–2332 (2012).
- Sheldon RA, Enzyme immobilization: the quest for optimum performance. *Adv Synth Catal* **349**:1289–1307 (2007).
- Smidsrød O and Skjåk-Bræk G, Alginate as immobilization matrix for cells. *Trends in Biotechnol* **8**:71–78 (1990).
- Elnashar MM, Danial EN and Awad GE, Novel carrier of grafted alginate for covalent immobilization of inulinase. *Indus Eng Chem Res* **48**:9781–9785 (2009).
- Gülay S and Şanlı-Mohamed G, Immobilization of thermoalkalophilic recombinant esterase enzyme by entrapment in silicate coated Ca-alginate beads and its hydrolytic properties. *Int J Biol Macromol* **50**:545–551 (2012).
- Levy MC and Edwards-Levy F, Coating alginate beads with cross-linked biopolymers: a novel method based on a transacylation reaction. *J Microencapsul* **13**:169–183 (1996).
- Matricardi P, Meo CD, Coviello T and Alhaique F, Recent advances and perspectives on coated alginate microspheres for modified drug delivery. *Expert Opin Drug Deliv* **5**:417–425 (2008).
- Hwang ET, Lee H, Kim JH, Tatavarty R and Gu MB, Highly-stable magnetically-separable organic-inorganic hybrid microspheres for enzyme entrapment. *J Mater Chem* **21**:6491–6493 (2011).
- Xu SW, Lu Y, Li J, Zhang YF and Jiang ZY, Preparation of novel silica-coated alginate gel beads for efficient encapsulation of yeast alcohol dehydrogenase. *J Biomater Sci Polym Ed* **18**:71–80 (2007).
- Huang H-Y, Tang Y-J, King V-A-E, Chou JW and Tsen JH, Properties of *Lactobacillus reuteri* chitosan-calcium-alginate encapsulation under simulated gastrointestinal conditions. *Int Microbiol* **18**:61–69 (2015).
- Li Y and McClements DJ, Controlling lipid digestion by encapsulation of protein-stabilized lipid droplets within alginate-chitosan complex coacervates. *Food Hydrocolloids* **25**:1025–1033 (2011).
- Nadavala SK, Swayampakula K, Boddur VM and Abburi K, Biosorption of phenol and o-chlorophenol from aqueous solutions on to chitosan-calcium alginate blended beads. *J Hazard Mater* **162**:482–489 (2009).
- Kim WT, Chung H, Shin IS, Yam KL and Chung DH, Characterization of calcium alginate and chitosan-treated calcium alginate gel beads entrapping allyl isothiocyanate. *Carbohydr Polym* **71**:566–573 (2008).
- Hari PR, Chandu T and Sharma CP, Chitosan/calcium-alginate beads for oral delivery of insulin. *J Appl Polym Sci* **59**:1795–1801 (1996).
- Bornscheuer UT, Microbial carboxyl esterases: classification, properties and application in biocatalysis. *FEMS Microbiol Rev* **733**:1–9 (2002).
- Panda T and Gowrishankar BS, Production and applications of esterases. *Appl Microbiol Biotechnol* **67**:160–169 (2005).
- Khanna S, Sekhon KK and Prakash NT, Cloning and expression of a biosurfactant gene from endosulfan degrading *Bacillus* sp.: correlation between esterase activity and biosurfactant production. *Biotechnology* **8**:235–241 (2009).
- Kim SB, Lee W and Ryu YW, Cloning and characterization of thermostable esterase from *Archaeoglobus fulgidus*. *J Microbiol* **46**:100–107 (2008).
- Ewis HE, Abdelal AT and Lu CD, Molecular cloning and characterization of two thermostable carboxyl esterases from *Geobacillus stearothermophilus*. *Gene* **329**:187–195 (2004).
- Kademi A, Abdelkader NA, Fakhreddine L and Baratti JC, A thermostable esterase activity from newly isolated moderate thermophilic bacterial strains. *Enzyme Microb Technol* **24**:332–338 (1999).
- Da Silva RR, Agricultural enzymes, phosphatases, peptidases, and sulfatases and the expectations for sustainable agriculture. *J Agric Food Chem* **67**:4395–4396 (2019).
- Bhatt P, Bhatt K, Huang Y, Lin Z and Chen S, Esterase is a powerful tool for the biodegradation of pyrethroid insecticides. *Chemosphere* **244**:125507 (2020).

- 27 Bayramoglu G and Arica MY, Immobilization of *Mucor miehei* esterase on core-shell magnetic beads via adsorption and covalent binding: application in esters synthesis. *Fibers Polym* **15**:2051–2060 (2014).
- 28 Ren G and Yu H, Oriented adsorptive immobilization of esterase BioH based on protein structure analysis. *Biochem Eng J* **53**:286–291 (2011).
- 29 Li R, Jiang L, Ye L, Lu J and Yu H, Oriented covalent immobilization of esterase BioH on hydrophilic-modified Fe<sub>3</sub>O<sub>4</sub> nanoparticles. *Biotechnol Appl Biochem* **61**:603–610 (2014).
- 30 Fan X, Liang W, Li Y, Li H and Liu X, Identification and immobilization of a novel cold-adapted esterase, and its potential for bioremediation of pyrethroid-contaminated vegetables. *Microb Cell Fact* **16**:149 (2017). <https://doi.org/10.1186/s12934-017-0767-9>.
- 31 Yavuz E, Gunes H, Harsa S and Yenidunya AF, Identification of extracellular enzyme producing thermophilic bacilli from Balcova (Agamemnon) geothermal site by ITS rDNA RFLP. *J Appl Microbiol* **97**:810–817 (2004).
- 32 Tekedar HC and Şanlı-Mohamed G, Molecular cloning, over expression and characterization of thermoalkalophilic esterases isolated from *Geobacillus* sp. *Extremophiles* **15**:203–211 (2011).
- 33 Laemmli UK, Cleavage of structural proteins during the assembly of the head of bacteriophage T4. *Nature* **227**:680–685 (1970).
- 34 Bradford MM, A rapid and sensitive method for the quantitation of microgram quantities of protein utilizing the principle of protein-dye binding. *Anal Biochem* **72**:248–254 (1976).
- 35 İlgü H, Turan T and Şanlı-Mohamed G, Preparation, characterization and optimization of chitosan nanoparticles as carrier for immobilization of thermophilic recombinant esterase. *J Macromol Sci, Part A* **48**:713–721 (2011).
- 36 Boyacı E, Eroğlu AE and Shahwan T, Sorption of As(V) from waters using chitosan and chitosan-immobilized sodium silicate prior to atomic spectrometric determination. *Talanta* **80**:1452–1460 (2010).
- 37 Dorati R, De Trizio A, Genta I, Merelli A, Modena T and Conti B, Gentamicin-loaded thermosetting hydrogel and moldable composite scaffold: formulation study and biologic evaluation. *J Pharm Sci* **106**:1596–1607 (2017).
- 38 Lai WF, Wong E and Wong WT, Multilayered composite-coated ionically crosslinked food-grade hydrogel beads generated from algal alginate for controlled and sustained release of bioactive compounds. *RSC Adv* **10**:44522–44532 (2020).
- 39 Zhou M, Lin F, Li W, Shi L, Li Y and Shan G, Development of nanosilver doped carboxymethyl chitosan-polyamideamine alginate composite dressing for wound treatment. *Int J Biol Macromol* **166**:1335–1351 (2021).
- 40 Tamimi M, Rajabi S and Pezeshki-Modaress M, Cardiac ECM/chitosan/alginate ternary scaffolds for cardiac tissue engineering application. *Int J Biol Macromol* **164**:389–402 (2020).
- 41 Saloglu D, Influence of lipase in swelling behavior of hydrogel, morphological properties of hydrogels and enzymatic polymerization reaction of PCL by using lipase immobilized hydrogels. *Res J Biotechnol* **12**:61–69 (2017).
- 42 Park H and Kim D, Swelling and mechanical properties of glycol chitosan/poly(vinyl alcohol) IPN-type superporous hydrogels. *J Biomed Mater Res, Part A* **78**:662–667 (2006).
- 43 Rahman MA, Culsum U, Kumar A, Gao H and Hu N, Immobilization of a novel cold active esterase onto Fe<sub>3</sub>O<sub>4</sub> approximately cellulose nanocomposite enhances catalytic properties. *Int J Biol Macromol* **87**:488–497 (2016).
- 44 Kolling DJ, Suguino WA, Angonesi Brod FC and Maisonnave Arisi AC, Immobilization of a recombinant esterase from *Lactobacillus plantarum* on polypropylene accurel MP1000. *Appl Biochem Biotechnol* **163**:304–312 (2011).
- 45 Dong F, Tang X, Yang X, Lin L, He D, Wei W *et al.*, Immobilization of a novel EST<sub>BAS</sub> esterase from *Bacillus altitudinis* onto an epoxy resin: characterization and regioselective synthesis of chloramphenicol palmitate. *Catalysts* **9**:620 (2019).
- 46 Ye L, Liu X, Shen GH, Li SS, Luo QY, Wu HJ *et al.*, Zhang, properties comparison between free and immobilized wheat esterase using glass fiber film. *Int J Biol Macromol* **125**:87–91 (2019).
- 47 Sharma A, Sharma T, Meena KR, Kumar A and Kanwar SS, High throughput synthesis of ethyl pyruvate by employing superparamagnetic iron nanoparticles-bound esterase. *Process Biochem* **71**:109–117 (2018).
- 48 Divakar K, Prabha S and Gautam P, Purification, immobilization and kinetic characterization of GxSxG esterase with short chain fatty acid specificity from *Lysinibacillus fusiformis* AU01. *Biocatal Agric Biotechnol* **12**:131–141 (2017).
- 49 Lee H, Jeong HK, Han J, Chung HS, Jang SH and Lee CW, Increased thermal stability of cold-adapted esterase at ambient temperatures by immobilization on graphene oxide. *Bioresour Technol* **148**:620–623 (2013).
- 50 Kim Y, Ryu BH, Kim J, Yoo W, An DR, Kim BY *et al.*, Characterization of a novel SGNH-type esterase from *Lactobacillus plantarum*. *Int J Biol Macromol* **96**:560–568 (2017).
- 51 Sungkeeree P, Whangsuk W, Sallabhan R, Dubbs J, Mongkolsuk S and Loprasert S, Efficient removal of toxic phthalate by immobilized serine-type aldehyde-tagged esterase G. *Process Biochem* **63**:60–65 (2017).
- 52 Yang L, Li X, Li X, Su Z, Zhang C, Xu M *et al.*, Improved stability and enhanced efficiency to degrade chlorimuron-ethyl by the entrapment of esterase SulE in cross-linked poly( $\gamma$ -glutamic acid)/gelatin hydrogel. *J Hazard Mater* **287**:287–295 (2015).
- 53 Yoo W, Le LTHL, Lee JH, Kim KK and Kim TD, A novel enantioselective SGNH family esterase (*NmSGNH1*) from *Neisseria meningitidis*: characterization, mutational analysis, and ester synthesis. *Biochim Biophys Acta, Mol Cell Biol Lipids* **1864**:1438–1448 (2019).
- 54 Samoylova YV, Sorokina KN, Piligaev AV and Parmon VN, Preparation of stable cross-linked enzyme aggregates (CLEAs) of a *Ureibacillus thermosphaericus* esterase for application in malathion removal from wastewater. *Catalysts* **8**:154 (2018).
- 55 Kwon S, Yoo W, Kim YO, Kim KK and Kim TD, Molecular characterization of a novel family VIII esterase with  $\beta$ -lactamase activity (*PsEstA*) from *Paenibacillus* sp. *Biomolecules* **9**:786 (2019).
- 56 Zheng GW, Yu HL, Li CX, Pan J and Xu JH, Immobilization of *Bacillus subtilis* esterase by simple cross-linking for enzymatic resolution of dl-menthyl acetate. *J Mol Catal B: Enzym* **70**:138–143 (2011).
- 57 Mohapatra BR, Gould WD, Dinardo O, Papavinasam S, Koren DW and Revie RW, Effect of immobilization on kinetic and thermodynamic characteristics of sulfide oxidase from arthrobacter species. *Prep Biochem Biotechnol* **38**:61–73 (2008).
- 58 Zhang YW, Prabhu P and Lee JK, Alginate immobilization of recombinant *Escherichia coli* whole cells harboring l-arabinose isomerase for l-ribose production. *Bioprocess Biosyst Eng* **33**:741–748 (2010).
- 59 Doraiswamy N, Sarathi M and Pennathur G, Cross-linked esterase aggregates (CLEAs) using nanoparticles as immobilization matrix. *Prep Biochem Biotechnol* **49**:270–278 (2019).
- 60 Le LTHL, Yoo W, Jeon S, Kim KK and Kim TD, Characterization and immobilization of a novel SGNH family esterase (*LaSGNH1*) from *Lactobacillus acidophilus* NCFM. *Int J Mol Sci* **21**:91 (2020).